Gene Augmentation Therapy Restores Retinal Function and Visual Behavior in a Sheep Model of *CNGA3* Achromatopsia

Eyal Banin[1], Elisha Gootwine[2], Alexey Obolensky[1], Raaya Ezra-Elia[3], Ayala Ejzenberg[1], Lina Zelinger[1], Hen Honig[2], Alexander Rosov[2], Esther Yamin[1], Dror Sharon[1], Edward Averbukh[1], William W Hauswirth[4] and Ron Ofri[3]

[1]Department of Ophthalmology, Hadassah-Hebrew University Medical Center, Jerusalem, Israel; [2]Agricultural Research Organization, The Volcani Center, Bet Dagan, Israel; [3]Koret School of Veterinary Medicine, Hebrew University of Jerusalem, Rehovot, Israel; [4]Department of Ophthalmology, University of Florida, Gainesville, Florida, USA

Achromatopsia is a hereditary form of day blindness caused by cone photoreceptor dysfunction. Affected patients suffer from congenital color blindness, photosensitivity, and low visual acuity. Mutations in the *CNGA3* gene are a major cause of achromatopsia, and a sheep model of this disease was recently characterized by our group. Here, we report that unilateral subretinal delivery of an adeno-associated virus serotype 5 (AAV5) vector carrying either the mouse or the human intact *CNGA3* gene under the control of the red/green opsin promoter results in long-term recovery of visual function in *CNGA3*-mutant sheep. Treated animals demonstrated shorter maze passage times and a reduced number of collisions with obstacles compared with their pretreatment status, with values close to those of unaffected sheep. This effect was abolished when the treated eye was patched. Electroretinography (ERG) showed marked improvement in cone function. Retinal expression of the transfected human and mouse *CNGA3* genes at the mRNA level was shown by polymerase chain reaction (PCR), and cone-specific expression of CNGA3 protein was demonstrated by immunohistochemisrty. The rescue effect has so far been maintained for over 3 years in the first-treated animals, with no obvious ocular or systemic side effects. The results support future application of subretinal AAV5-mediated gene-augmentation therapy in *CNGA3* achromatopsia patients.

Received 5 February 2015; accepted 5 June 2015; advance online publication 21 July 2015. doi:10.1038/mt.2015.114

INTRODUCTION

Congenital achromatopsia (ACHM) is a hereditary retinal disease characterized by loss of cone function. Affected patients are legally blind from birth, suffering from severe impairment of visual acuity and loss of color vision, as well as hemeralopia (inability to see as distinctly in bright light as in reduced illumination), nystagmus and extreme photosensitivity. In cases of complete ACHM, only rod vision is present[1] (**Supplementary Figure S1**).

ACHM is recessively inherited, with a prevalence of approximately 1 in 30,000.[2] In most cases, it is caused by mutations in the cyclic nucleotide-gated (CNG) ion channel subunit A3 (α subunit)[3,4] or B3 (β subunit) of cone photoreceptors.[5–7] Studies performed mainly in North American and European populations have shown that mutations in the *CNGB3* gene are the most common cause of ACHM, accounting for at least 50% of all cases.[7,8] Mutations in *CNGA3* account for approximately 25% of cases,[4] though in some populations, including Israeli and Palestinian patients, mutations in *CNGA3* are the most common cause of ACHM.[9] Interestingly, recent reports suggest that *CNGA3* mutations are a relatively common cause of ACHM in the Chinese population as well.[10,11] Mutations in three additional genes, *GNAT2*, *PDE6C*, and *PDE6H* have also been identified as rare causes of the disease.[12–14]

Several dog breeds, including the Alaskan malamute, German shorthaired pointer and miniature Australian shepherd, also suffer from ACHM. The canine disease is a *CNGB3* channelopathy, caused by either a genomic deletion ($CNGB3^{-/-}$) or a missense mutation ($CNGB3^{m/m}$).[15,16] Consequently, the dog serves as a naturally occurring large animal model for human *CNGB3* ACHM.[17,18]

In 2010, we reported appearance of congenital day blindness in the Improved Awassi sheep breed in Israel.[19] This autosomal-recessive hereditary disease was determined to be caused by a C→T substitution leading to a premature stop codon at residue 236 (c.706C>T, p.R236*) of the ovine *CNGA3* gene,[20] thus providing a naturally occurring large animal model for human *CNGA3*-related ACHM.

As cones are responsible for some of the most important attributes of human vision, including visual acuity and color perception, there is a great impetus to develop therapies for patients affected by hereditary cone dystrophies and degenerations. Thus far, gene-augmentation therapy has been reported in murine

This study was performed in Bet Dagan and in Jerusalem, Israel.

Correspondence: *Eyal Banin, Center for Retinal and Macular Degenerations, Department of Ophthalmology, Hadassah-Hebrew University Medical Center, Jerusalem, Israel. E-mail: banine@mail.huji.ac.il*

Table 1 Age, treatment, and follow-up of experimental animals treated with BSS alone or with AAV5 vectors carrying the GFP reporter gene, mouse *CNGA3*, or human *CNGA3* genes

Animal No. (A-affected N-normal)	Age at surgery (months)	Sex	Viral dose (VG•10^{11})	Bleb volume (µl)	Post-op maze testing		Post-op ERG testing	
					Number of tests	Follow-up duration (months)	Number of tests	Follow-up duration (months)
BSS alone								
3895 (A)	4	F	-	500	3	6	2	6
GFP reporter gene								
4735 (N)	7	F	11.1	600	5	6	2	6
4847 (N)	7	F	12.0	650	3	3	2	5
5304 (N)	5	M	4.7	500	2	4	2	4
Mouse *CNGA3*								
4056 (A)	4	M	12.0	500	13	37	5	32
4019 (A)	6	F	14.4	600	10	35	5	30
3909 (A)	6	F	6.5	500	11	35	5	30
4855 (A)	6	M	7.1	600	9	24	3	19
2874 (A)	31	M	3.0	500	2	4	2	4
2998 (A)	31	F	3.0	500	2	4	2	4
3350 (A)	24	F	2.4	400	2	4	2	4
8412 (A)	56	F	3.0	500	1	4	2	4
Human *CNGA3*								
4954 (A)	6	F	6.4	500	10	24	3	22
4984 (A)	5	M	5.8	450	10	24	3	19
4826 (A)	7	F	6.4	500	10	24	3	22
4624 (A)	10	M	5.1	~400	10	23	3	17
5187 (A)	9	F	4.5	550	5	18	2	9
2875 (A)	31	M	3.2	500	6	14	3	14
5066 (A)	10	F	2.6	400	4	10	2	9
5067 (A)	10	F	3.0	450	4	10	2	9

AAV, adeno-associated virus; BSS, balanced salt solution; ERG, electroretinography; GFP, green fluorescent protein.

models of *CNGB3*,[21] *CNGA3*[22–24] and *GNAT2*[25] ACHM, and in the canine *CNGB3* ACHM models.[18] In many of these models, we have shown that adeno-associated virus serotype 5 (AAV5) vectors carrying the appropriate gene markedly improve cone function.[18,24,25] Moreover, we have published that AAV5 vectors target cones effectively and therapeutically also in monkeys.[26]

Like the dog and the human eye, and unlike murine models of ACHM, the sheep possesses a cone-rich retina.[27] In addition, the similarity of the globe size to that of humans makes it a more relevant model for testing and assessing the effects of localized subretinal surgical delivery of the viral vector. Less than 10 years ago, Leber's congenital amaurosis (LCA) became the first inherited retinal disease for which clinical gene-augmentation therapy trials were approved.[28] This approval was granted, to a large extent, based on positive results of gene-augmentation studies in *RPE65*-mutant dogs,[29–31] thus reinforcing the advantages of a naturally occurring large animal model in the evolution of this treatment modality for blind patients. The purpose of the present study was to evaluate the efficacy of AAV5 vector-mediated *CNGA3* gene-augmentation therapy in our ACHM ovine model using behavioral, electrophysiological, structural and molecular methodologies, with the aim of applying similar treatment in *CNGA3*-related ACHM patients in the future.

RESULTS

The intervention

Affected sheep, homozygous for the *CNGA3* mutation,[20] were treated unilaterally with a subretinal injection of AAV5 vector containing either the normal mouse (m) or the normal human (h) *CNGA3* gene under control of the 2.1 red/green opsin promoter. Three unaffected sheep received a subretinal injection of a similar vector carrying the green fluorescent protein (GFP) marker gene. In one *CNGA3*-mutant animal, subretinal injection of the vehicle solution (balanced salt solution (BSS)) alone was performed.

For animal and treatment details, see Materials and Methods section, **Table 1** and **Supplementary Figure S2**. Systemic recovery from surgery was unremarkable in all 20 operated animals. The subretinal bleb formed by the injection resorbed within 24 hours in all eyes. A focal cataract was found in one operated eye (sheep 3909) due to intraoperative trauma to the lens. Mild anterior uveitis, which resolved within a few days, was seen in two operated

Table 2 Behavioral maze testing

Treatment	Passage time (seconds)	Collisions (*n*)
Control unaffected	5.6 ± 0.5[a]	0.0 ± 0.1[a]
CNGA3-mutant untreated	25.6 ± 0.7[c]	5.3 ± 0.1[c]
CNGA3-mutant treated with mouse *CNGA3*	7.4 ± 0.4[b]	0.2 ± 0.1[a,b]
CNGA3-mutant treated with human *CNGA3*	8.2 ± 0.6[b]	0.2 ± 0.1[b]

Average photopic maze passage time and number of collisions for unaffected control sheep, *CNGA3*-mutant sheep and *CNGA3*-mutant treated with viral vectors containing either the mouse (m) or human (h) *CNGA3* cDNA. The first post-treatment maze testing session was conducted 1–2 months after surgery, and periodic retesting sessions were subsequently conducted, with some animals tested in up to 11 sessions, and as long as 37 months postoperatively. Data presented as least squares means ± standard error. Within a trait, mean values followed by different letters are significantly different at $P < 0.05$ (i.e., a significantly differs from b, b from c, and a from c).

eyes (sheep 4855, 4984). Long-term follow up by board certified specialists in ovine medicine and veterinary ophthalmology did not reveal any signs of systemic or ocular complications, and funduscopic appearance of control and operated eyes was clinically indistinguishable.

Behavioral assessment

Under scotopic conditions, both unaffected and *CNGA3*-mutant sheep navigated a two barrier maze with a similar ($P > 0.05$) passage time of 5.6 ± 0.4 seconds, and no collisions. Under photopic conditions, control unaffected animals navigated the maze in 5.6 ± 0.5 seconds with practically no collisions. Both passage time and number of collisions of untreated *CNGA3*-mutant sheep were significantly ($P < 0.001$) higher, being 25.6 ± 0.7 seconds and 5.3 ± 0.1 collisions, respectively (**Table 2**). Session number, gender, trial repetition number, or age at time of testing had no significant effect on the behavioral parameters.

Following gene-augmentation therapy, all operated sheep treated with vectors containing either m*CNGA3* or h*CNGA3* were able to navigate the maze under photopic conditions with passage times and collisions number that were close to, but still significantly different ($P < 0.05$) from those of unaffected control sheep (**Table 2**, **Supplementary Movie S1**). This behavioral improvement in the treated sheep was already observed at the first postoperative maze test, conducted 1–2 months after surgery, and was maintained for more than 3 years postoperatively in the earliest-treated animals (**Figure 1a–c**). The ability of treated animals to navigate the maze was unaffected when their left (untreated) eye was patched; however, patching the right (treated) eye abolished the treated animals' ability to navigate the maze (**Figure 1d,e** and **Supplementary Movie S1**). A *CNGA3*-mutant animal injected with BSS alone was tested three times over the span of 6 months postsurgery and failed to navigate through the maze in all the behavioral tests (passage time over 30 seconds), in similarity to the performance of untreated affected sheep (**Supplementary Figure S3a**).

Electroretinography (ERG)

ERG recordings showed marked long-term improvement in cone function following either m*CNGA3*- or h*CNGA3*-augmentation therapy in affected sheep (**Figure 2**). Representative 30–80 Hz (10 cd•s/m^2) flicker responses of m*CNGA3*- and h*CNGA3*-treated sheep are shown in **Figure 2a**, where a significant increase in response amplitudes is seen following treatment. At the three highest stimulus intensities (2.5, 5, and 10 cd•s/m^2), critical flicker fusion frequency (CFFF) values of the operated eye were significantly higher than pretreatment baseline values in both m*CNGA3*- and h*CNGA3*-treated sheep ($P \leq 0.05$, **Figure 2b**). Furthermore, at all four stimulus intensities, flicker amplitudes of treated eyes were higher than pretreatment baseline values and higher than responses of the untreated fellow eye, attaining statistical significance at the highest stimulus intensity ($P = 0.03$ in both m*CNGA3*- and h*CNGA3*-treated eyes, **Figure 2c**). Two ERG recordings up to 6 months post-surgery in the affected animal injected with BSS alone failed to show any improvement in cone ERG (**Supplementary Figure S3b**).

Molecular genetics analysis

We previously reported that mutant *CNGA3* transcript is expressed in the retinas of affected (day-blind) sheep.[20] RT-PCR analysis performed in this study on mRNA samples isolated from unaffected control and affected *CNGA3*-mutant animals revealed the previously reported major transcript, as well as another, minor transcript in which exons 5–8 (including the mutation site) are skipped (**Figure 3a**).

Treatment of *CNGA3*-mutant animals with either m*CNGA3* or h*CNGA3* resulted in successful retinal transfection that was confirmed by RT-PCR analysis followed by Sanger sequencing showing the presence of mouse and human-specific mRNA sequences (**Figure 3b**).

Histology and immunohistochemistry

Unaffected control sheep retinas stained with anti-CNGA3 antibody demonstrated protein expression in the inner and outer segments of cone photoreceptors (**Figure 4a**), while no CNGA3 expression was seen in retinas of untreated *CNGA3*-mutant sheep (**Figure 4b**). As expected, in unaffected sheep, red/green opsin staining was limited to the cone outer and inner segments. Interestingly, some degree of red/green opsin mislocalization to the cone cell bodies and synaptic regions was observed in the retinas of affected *CNGA3*-mutant sheep (**Figure 4b**, third panel).

To test transfection efficacy, an AAV5 vector carrying the GFP reporter gene under the control of the same red/green opsin promoter used in the *CNGA3*-carrying vectors was produced and injected into the subretinal space of three unaffected sheep. Histological sections were then immunohistostained with anti-GFP antibody. In **Figure 4c**, strong cone-specific GFP expression can be seen in the treated area, colocalizing with red/green opsin.

In both m*CNGA3*- and h*CNGA3*-treated retinas from *CNGA3*-mutant sheep, immunohistostaining showed expression of the CNGA3 protein, largely colocalized with red/green opsin (**Figure 4d,e**). No CNGA3 labeling was found in the fellow, untreated eyes (data not shown). H&E histology performed after gene-augmentation treatment showed normal retinal architecture with no signs of retinal damage or postoperative complications (**Supplementary Figure S4**).

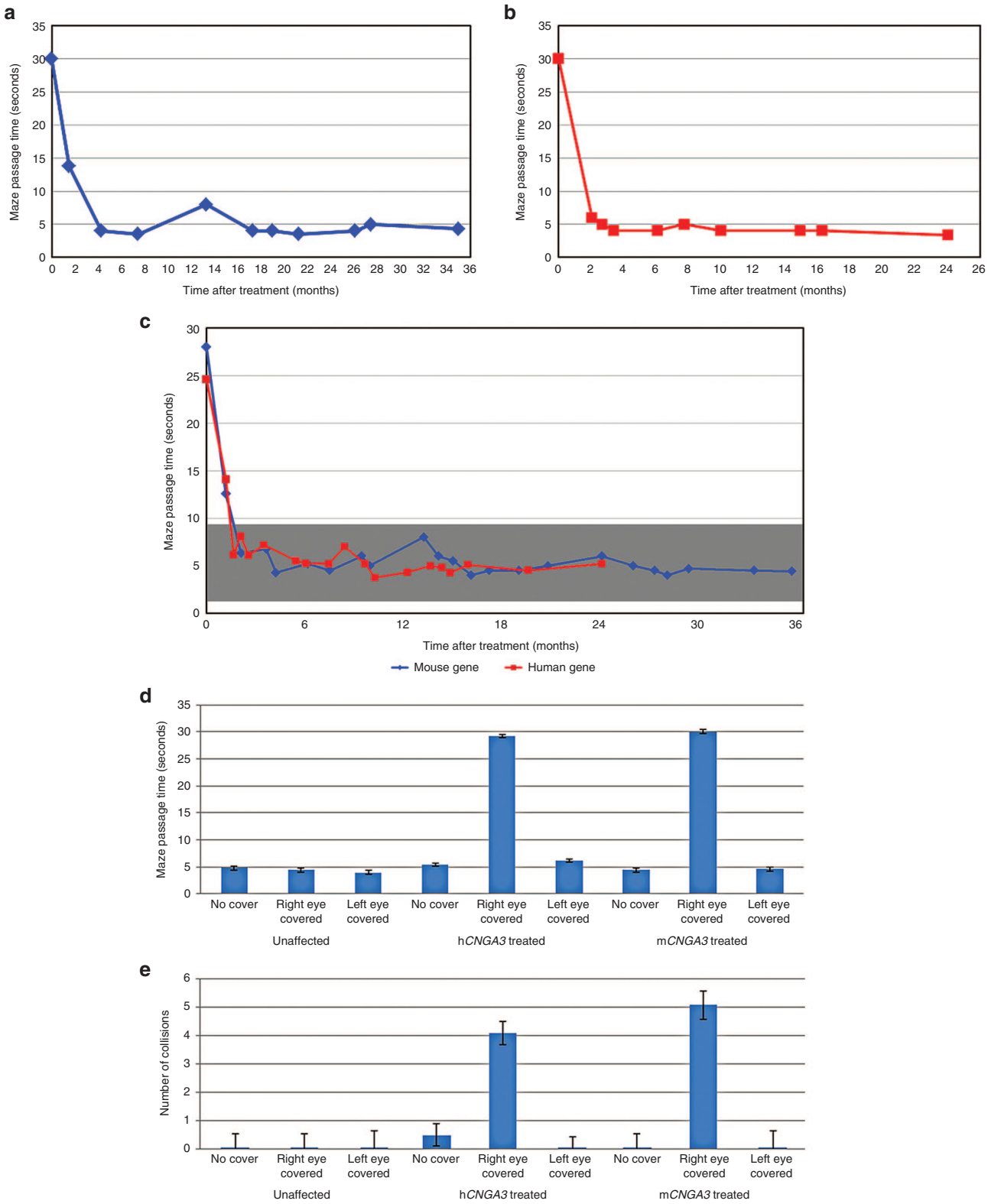

Figure 1 Photopic maze passage time before ("day 0") and after gene-augmentation therapy. (**a**) Sheep no. 3909 was treated with an AAV5 vector containing mouse (m) *CNGA3*. (**b**) Sheep no. 4984 was treated with a vector containing human (h) *CNGA3*. (**c**) Average passage time for sheep treated with viral vectors containing either m*CNGA3* (blue) or h*CNGA3* (red). Each post-treatment data point represents the mean passage time of up to six animals. Gray background represents passage time of normal unaffected sheep (mean ± 2 SD, $n = 20$). Please note that as treatment with the mouse gene was initiated before using the human gene (see study design), the follow up time for animals treated with the mouse gene was longer. (**d,e**) Maze navigation time (**d**) and number of collisions (**e**) following alternate eye patching in unaffected control sheep ($n = 4$) and *CNGA3*-mutant sheep treated in their right eye with an AAV5 vector carrying either the human ($n = 8$) or the mouse ($n = 4$) *CNGA3* gene.

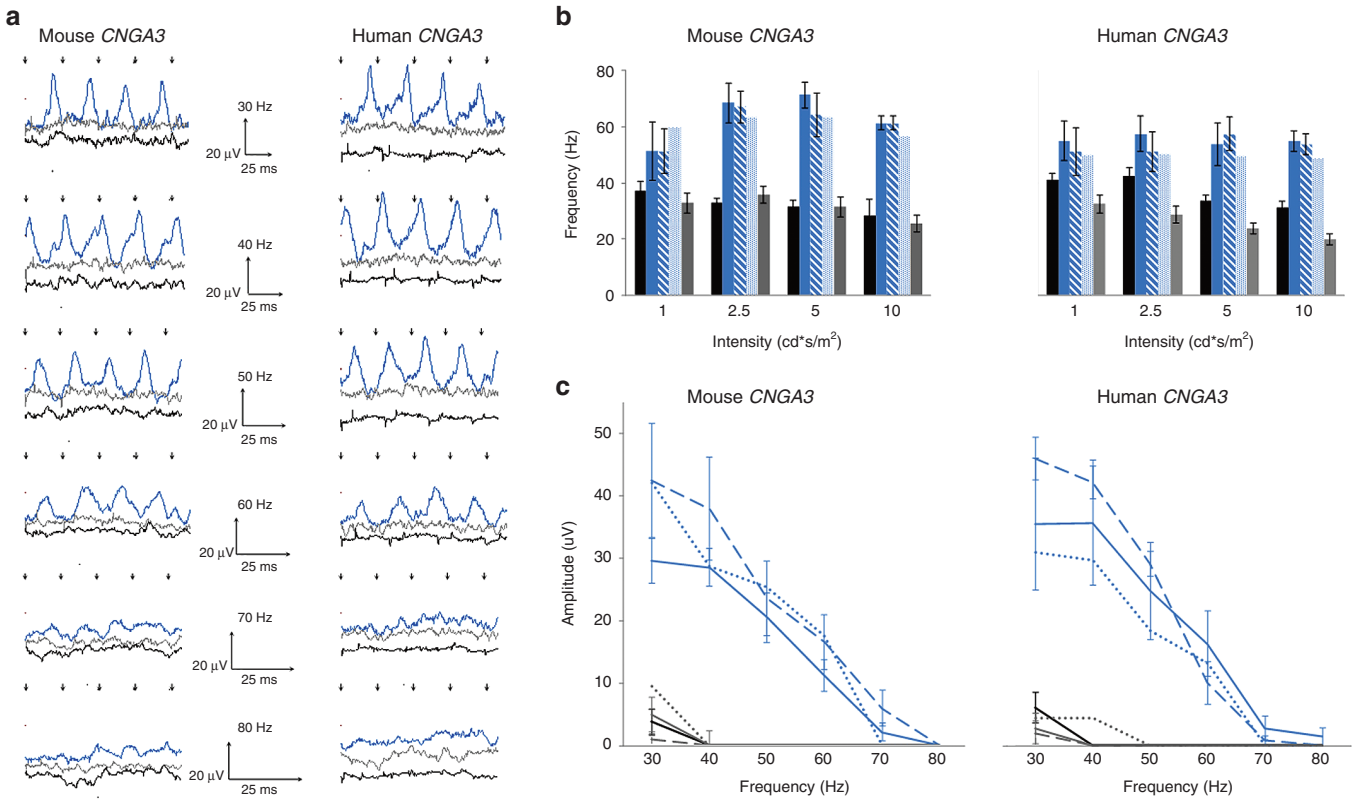

Figure 2 Photopic electroretinography (ERG) responses. (**a**) Cone flicker tracings (30–80 Hz, 10 cd•s/m^2) of representative *CNGA3*-mutant sheep eyes treated with mouse (m) (sheep 2998, left panel) or human (h) (sheep 2875, right panel) *CNGA3* showing functional efficacy of treatment. Following treatment, marked increase of cone flicker amplitudes was observed in treated eyes. Black tracing: baseline preoperative recording; blue and gray tracings: postoperative recording in treated (blue) and nontreated fellow (gray) eyes. Postoperative recordings were conducted at 4 and 14 months post-op for the m*CNGA3*- and h*CNGA3*-treated animals, respectively. Flash stimulus onset is shown by arrows. (**b**) Critical flicker fusion frequency (CFFF) of *CNGA3*-mutant sheep treated with mouse (left) and human (right) *CNGA3*. For both treatments, CFFF values at the three highest stimulus intensities were significantly higher in the treated eyes compared to both the baseline values and the untreated fellow eyes at the first and second follow-up recordings ($P \leq 0.05$). Black bars: baseline preoperative CFFF at the four intensities tested; blue bars: first post-op (~2 months) recording ($n = 8$ in each treatment group); blue hash-marked bars: second post-op recording (4.6±1.2 months for m*CNGA3* and 7.6±1.2 months for h*CNGA3*, $n = 8$ in each treatment group); dotted blue bars: last recording performed to date (30.4±1.5 months for m*CNGA3* and 16.5±2.1 months for h*CNGA3*, $n = 3$ in each treatment group); gray bars: CFFF values of the nontreated fellow eye at the first follow-up. Results are presented as mean ± SE, in Hz; last follow-up recording could not be statistically analyzed due to small number of recorded animals. (**c**) Cone flicker responses of *CNGA3*-mutant sheep treated with mouse (left) and human (right) *CNGA3*. Following gene-augmentation therapy, cone flicker responses significantly improved in both m*CNGA3*- and h*CNGA3*-treated eyes. Effect of treatment was statistically significant ($P \leq 0.05$), and was maintained over the course of follow-up in both groups. Black lines: baseline preoperative flicker amplitudes; blue, dashed blue and dotted blue lines: flicker amplitudes in treated eyes at the first, second and last follow-up, respectively, with recording intervals and number of animals identical to those detailed for panel **b**. Responses of the nontreated fellow eyes recorded in the same sessions are shown in gray, dashed gray, and dotted gray lines, respectively. Responses to the 10 cd•s/m^2 flicker stimulus are plotted as a function of the stimulating frequency (Hz), and results are presented as mean ± SE, in µV.

DISCUSSION

We report here that gene-augmentation therapy restores daytime vision and *CNGA3* expression, and significantly improves cone function in an ovine model of *CNGA3* ACHM, with long-term efficacy and no obvious signs of toxicity. Similar therapy by our group and others has resulted in the recovery of cone-mediated function in mouse models of the disease.[23,24,32] However, the present study is the first to report on such improvement in a naturally occurring, cone-rich large animal model of *CNGA3* ACHM. Restoration of cone function in the treated sheep was documented by both photopic behavioral maze testing and ERG recordings, with improvement already evident at the first postoperative assessment, 1–2 months after subretinal delivery of the AAV5 vector carrying *CNGA3*. The effect was long-lasting, as it is still present more than 3 years postoperatively in the earliest-treated animals. It is worth noting that treatment was applied only once, and that the subretinal injection covered only a limited part of the retina, yet this was enough to provide substantial behavioral and electrophysiological rescue. Scotopic ERG recordings were not performed in this study, as we previously demonstrated that rod function is preserved in *CNGA3*-mutant sheep[19] and the present study was mainly focused on determining whether gene augmentation therapy can restore cone function. Obviously, such scotopic recordings along with careful monitoring of additional systemic and ocular parameters will have to be conducted to demonstrate safety in future preclinical trials that will address dosing as well as toxicity using clinical-grade viral vectors.

The eye, and particularly the retina, is an ideal target for gene-augmentation therapy, as has been shown in many mouse and a number of canine models.[33] In humans, treatment of *RPE65*

LCA as well as X-linked choroideremia using AAV vectors has been shown to be effective and safe,[34,35] and human gene-augmentation therapy trials for Stargardt disease, Usher syndrome, and additional retinal conditions are ongoing.[36] ACHM is a very good target for gene augmentation, as the cones are largely preserved. Therefore, the therapeutic window may be wider than for other forms of hereditary retinal degeneration, such as LCA, in which loss of photoreceptors limits the applicability of this treatment modality. Accordingly, our study of *CNGA3* augmentation demonstrates a treatment effect in animals ranging in age from 3.6 to 55.6 months (the average life expectancy for sheep is between 10–12 years). On the other hand, in a similar trial in the canine *CNGB3* ACHM model, treatment was effective when delivered to dogs younger than 6 months of age, but was only minimally effective in dogs over 1 year of age.[18,37] It has been suggested that the reduced effect in older dogs may be due to an age-related loss of cone outer segments, an inability of the canine cones to reassemble the CNG channel, or a combination of both factors.[37] Our results suggest that the sheep and dog models of achromatopsia differ in this regard, despite their similar life span. We did not observe an age-related loss of outer segments in our model (for example, **Figure 4d,e**), and evidently also elderly sheep are able to assemble a functional CNG channel following gene augmentation therapy. It remains to be seen whether with respect to treatment human patients resemble the ovine or canine model, but studies in human ACHM patients using optical coherence tomography as well as adaptive optics suggest that rod and cone structure is relatively preserved. When disruption of retinal structure does occur in some patients, it is often localized to the IS/OS junction and does not necessarily correlate with age. Thus, specifically assessing retinal structure in a given patient (rather than age) may better guide application of gene augmentation therapy.[9,38,39]

The structural abnormalities present in the foveal area in some cases (also demonstrated in **Supplementary Figure S1h**) furthermore raise the important question of where in the retina to place a human subretinal injection and whether to include the fovea in the subretinal bleb that is formed. Surgical damage (macular hole and foveal thinning) caused by the detachment of residual foveal cones in patients with *RPE65*-LCA treated by gene augmentation therapy has been reported.[28,40] In contrast, similar subfoveal treatment in patients with choroideremia was not associated with such injury.[35] Regrettably, the sheep model cannot provide guidance on this issue; despite the fact that this is a cone-rich retina and a large eye, it does not possess a macula and a fovea. One option could be to place the subretinal injection adjacent to (rather than directly under) the fovea and thereby allow a pseudo-fovea to develop, as will be described below. Alternatively, the surgical approach could be tailored according to the specific structural findings in each patient, delivering the viral vector under the fovea only in those showing preserved foveal structure.

Efficacy in older animals and patients may be influenced by factors additional to survival of the target cells and success of transfection. In the case of complete ACHM, as seen in most human patients, significant cone-vision amblyopia is expected, as color and high-acuity vision are never experienced. Unlike

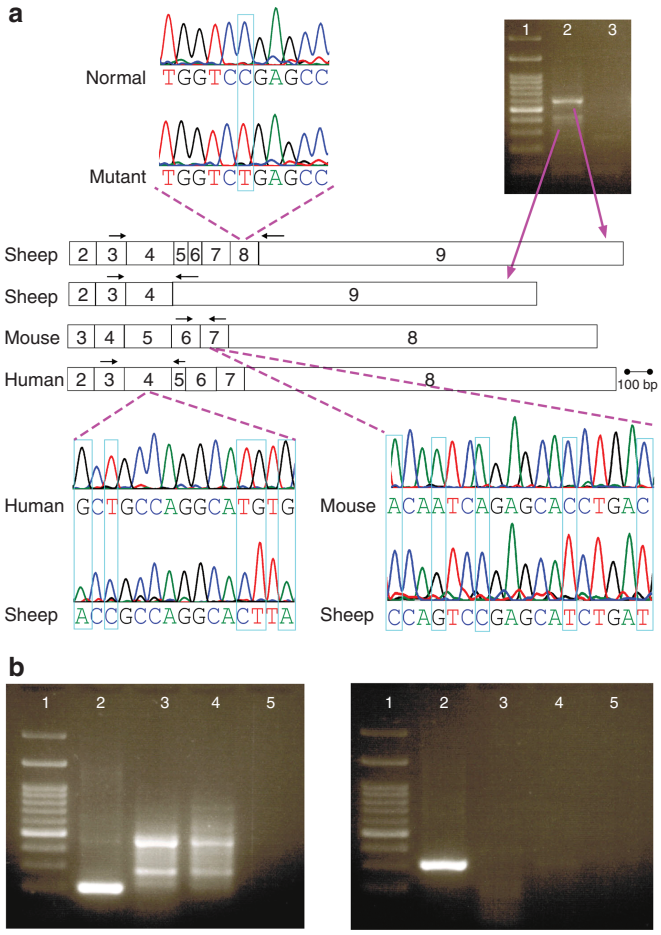

Figure 3 Molecular genetic analysis. (**a**) Transcripts of sheep, mouse, and human *CNGA*3 orthologs. The causative mutation in *CNGA3*-mutant sheep is located in exon 8 which is present in the major *CNGA*3 transcript, but is skipped (together with exons 5–7) in the novel minor transcript reported herein. The agarose gel (upper right panel: lane 1—molecular size marker, lane 2—reverse transcription–polymerase chain reaction (RT-PCR) products from a normal unaffected sheep retina, lane 3—double distilled water negative control) depicts RT-PCR products of a normal sheep retina (lane 2) using primers located in exons 3 and 9. Sanger-sequencing analysis revealed that the upper band represents the major *CNGA*3 transcript and the lower band represents the novel minor transcript in which exons 5 through 8 are skipped. The same RT-PCR pattern was observed in both normal and affected *CNGA3*-mutant sheep. The middle panel depicts the mRNA structure in different species. Note that since the full sequence of the sheep *CNGA3* gene is currently unknown, exon borders are deduced from those reported in the orthologous genes. Black arrows represent the location of the different primers that were designed to specifically amplify *CNGA3* mRNA of each of the three species (our analysis did not include the most 5′ exons 1 and 2). The chromatograms demonstrate parts of the mouse and human transcripts amplified from retinas of treated *CNGA3*-mutant, showing some of the sequence differences that distinguish them from the sheep sequence (highlighted in light blue boxes). (**b**) Agarose gel electrophoresis of RT-PCR products obtained following use of primers designed to amplify mouse (left panel) or human (right panel) *CNGA3* mRNA. Lane 1—molecular size marker, lane 2—retinal cDNA of *CNGA3*-treated affected sheep, lane 3—retinal cDNA of untreated *CNGA3*-mutant sheep, lane 4—retinal cDNA of untreated normal sheep, lane 5—double distilled water negative control. A specific band was obtained in lane 2 for both the human (~300 bp) and mouse (~200 bp) *CNGA*3 cDNA, and verified by sequencing. Lanes 3 and 4 in the left panel contain nonspecific amplification due to the lack of a specific template for PCR.

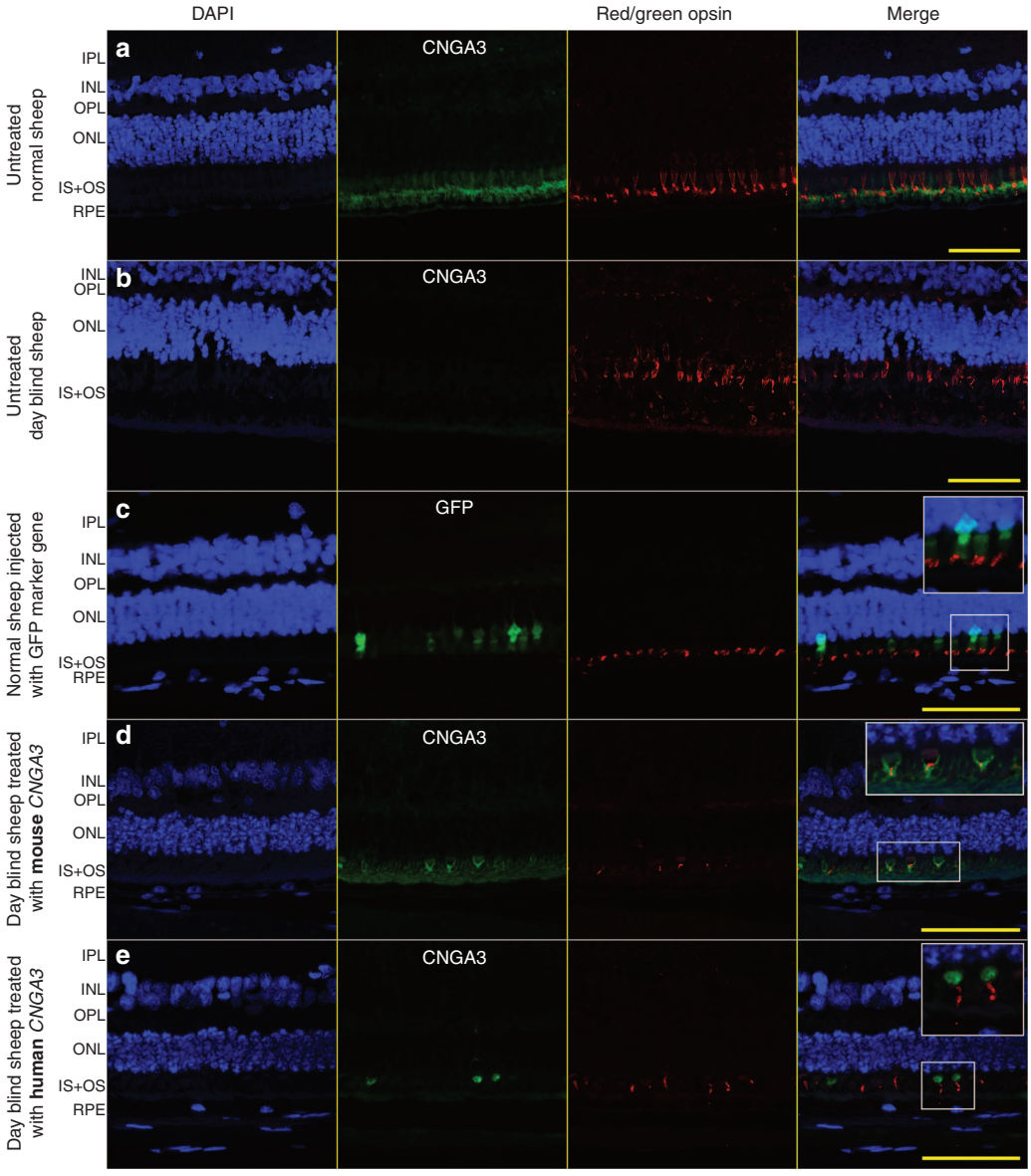

Figure 4 Gene-augmentation treatment restores CNGA3 protein expression in *CNGA3*-mutant sheep retinas. (**a**) Normal sheep retina. Anti-CNGA3 immunohistochemical staining shows strong protein expression in the outer segments of cone photoreceptors, colocalizing with red/green opsin (5-month-old animal). (**b**) No CNGA3 expression was observed in the retina of *CNGA3*-mutant day-blind sheep. Anti-red/green opsin staining revealed a large number of red/green cones in the retina, with some mislocalization of opsin to the cone cell bodies and synaptic region (5-month-old animal). (**c**) Unaffected sheep retina injected with an AAV5 vector carrying the green fluorescent protein (GFP) marker gene under control of the red/green opsin promoter. Double-labeling with anti-GFP and anti-red/green opsin antibodies showed strong GFP expression in the cell bodies and inner segments of red/green cones (age of animal at surgery 7 months, enucleated 6 months post-op). (**d,e**) *CNGA3*-mutant sheep retinas following gene-augmentation therapy with either mouse (**d**) or human (**e**) *CNGA3*. In both cases, CNGA3 protein was expressed, mainly in the outer segments of red/green cone photoreceptors (both animals 31 months old at surgery. Mouse *CNGA3*-treated enucleated 4 months post-op; Human *CNGA3*-treated enucleated 14 months post-op). INL, inner nuclear layer; IPL, inner plexiform layer; IS+OS, inner and outer segments of photoreceptors; ONL, outer nuclear layer; OPL, outer plexiform layer; RPE, retinal pigment epithelium. Nuclei are counterstained with 4′,6-diamidino-2-phenylindole (blue). Original magnification ×40. Scale bars = 50 µm.

ACHM patients, *CNGA3*-mutant sheep have residual cone function,[19,41] and this may allow at least partial development of cone-mediated cortical vision. Therefore, the augmentation of cone function at the retinal level by gene delivery might more easily manifest in behavioral functional improvements in treated sheep. The question of whether humans will respond in a similar manner remains open, but some lines of evidence do support plasticity of the central visual pathways in primates. For example, the addition of a third opsin by gene-augmentation therapy in adult monkeys who were red/green color-deficient from birth resulted in the development of trichromatic color vision behavior.[26] In humans, including elderly patients, some improvement in amblyopia was reported when the better seeing eye was lost and when certain novel visual rehabilitation paradigms were used.[42] In addition, recent studies in patients in which a visual prosthesis was implanted also suggest an ability to learn to use the novel

form of "vision" provided by these systems,[43] and abundant literature on sensory substitution as applied to the visual system provides further support for this type of plasticity.[44] Finally, in a number of *RPE65*-LCA patients treated by gene-augmentation therapy, a shift of visual fixation to the treated parafoveal retinal area was observed 9–12 months after treatment with preservation of light sensitivity restricted to the cortical projection zone of the newly formed pseudo-foveas.[45,46] Functional MRI studies in three other patients, including a 35-year-old, showed increased cortical activation upon visual stimulation of the treated versus untreated eye.[47,48] Similar development of a preferred extra-foveal retinal location that was accompanied by reorganization of visual processing was reported to occur in patients with macular degeneration, and specifically only after foveal function was lost in both eyes.[49] In preparation for gene-augmentation trials of ACHM in humans, this issue should be carefully addressed, and visual rehabilitation programs to "teach" the use of the newly available visual data emanating from the now-active cone photoreceptors should be considered.[42,50] Patients may be assessed by novel techniques, such as functional MRI, to follow possible activation/reorganization of visual pathways, and counseled that although the delivered gene may be expressed within a few short weeks, functional–behavioral visual benefits may take longer to manifest.

Sequence homology of the murine (NCBI Reference Sequence: NP_001028489.1) and human (NCBI Reference Sequence: XP_005252850.1) *CNGA3* genes to the ovine ortholog is 92 and 93%, respectively. Treatment with both mouse and human genes showed significant improvement in cone function and photopic behavior in the sheep model. Positive results are therefore also expected in human patients for whom the homology of the delivered gene would be complete. In addition, the red/green opsin promoter used here proved to be robust and specific, resulting in significant expression of the GFP reporter gene, as well as the murine and human *CNGA3* genes, within red/green cones in the area formed by the subretinal bleb during surgery.

As shown previously[19] and in the present study, *CNGA3*-mutant sheep fail their behavioral maze tests. However, ERG recordings demonstrate that their cone function is attenuated, but not absent.[19,41] This is in contrast to ERG recordings in most human ACHM patients in which cone function is usually undetectable.[51–54] The causative mutation in the affected sheep leads to the appearance of a premature stop codon at residue 236 of the ovine *CNGA3*,[20] precluding the expectation of a full-length, functional CNGA3 protein. While in most cases a mutant transcript that includes a premature stop codon would result in the activation of the nonsense-mediated mRNA-decay surveillance system that would then prevent the production of a short mutant protein, our previous analysis shows that the mutant transcript is present in the affected sheep retina.[20] We therefore predict that such a short mutant protein is present and might posses partial function that could be responsible for this discrepancy. *CNGA3* alternative-splice variants have been detected in humans,[4,55,56] and we report here that this also occurs in the sheep retina. The novel alternatively spliced transcript reported herein (lacking exons 5–8) is expected to produce a mutant protein lacking a relatively large portion of the native protein and it is therefore unlikely to be functional, although this could be a second possibility to explain the partial cone function seen in affected sheep. A third theoretical possibility to explain the very limited cone function in *CNGA3*-mutant sheep is the formation of a partially functional channel based on the CNGB3 subunit alone. To date, this has not been reported in any species, and functional CNG channels probably do not form in the absence of CNGA3.[57,58] However, it should be noted that in mice the opposite does occur, *i.e.*, partial function of irregular homomeric CNGA3 channels is seen in *CNGB3*-mutant animals.[59,60] The question whether a partially functional CNGB3-alone channel can form in sheep or whether CNGB3 can interact with the mutant CNGA3 or the short isoform of CNGA3 in the ovine retina need to be further investigated.

In conclusion, the results presented here support the concept of gene augmentation for *CNGA3* ACHM, with long-term, persistent improvement of photopic vision and cone function achieved in a wide age range of *CNGA3*-mutant sheep. While *CNGA3* ACHM is reportedly relatively rare in Western populations, findings in the Israeli population as well as recent reports in the Chinese population[10,11] suggest that this disease is not uncommon. The characteristics of ACHM make it an attractive target for gene therapy, and the outcomes of the present study taken together with the results in mouse and canine models of this disease may help pave the way to application of this treatment in patients.

MATERIALS AND METHODS

Study design. This was an open-label, nonrandomized observational study designed to detect possible differences between control and experimental (gene-augmentation-treated) eyes. Affected sheep, homozygous for the *CNGA3* mutation,[20] were treated unilaterally with a subretinal injection of AAV5 vector containing either the normal mouse ($n = 8$) or human ($n = 8$) *CNGA3* gene under control of the 2.1 red/green opsin promoter. Three unaffected sheep received a subretinal injection of a similar vector carrying the GFP marker gene. One affected animal was subretinaly injected with BSS solution alone and served as a vehicle control. Age at time of surgery and the treatment applied are presented in **Table 1**. This is an ongoing study that has not yet reached its endpoint, as animals are being maintained for longer-term follow-up, unless sacrificed for molecular genetic or histological analysis.

Initially, gene augmentation therapy was performed on animals 4–7 months of age, which are considered young animals. Once it became obvious that treatment at these ages is efficacious, we operated on animals older than 1 year, which are considered mature. In order to maximize the chance of observing an effect, high doses of the vector carrying the mouse gene (animals number 4056 and 4019, 12.0×10^{11} and 14.4×10^{11} viral genomes respectively) were initially deliverd (**Table 1**). Once an effect was seen with these doses, approximately half of the initial dose (animals number 3909, 4855) was used. When this also proved effective, we again reduced the dose by approximately half (animals number 2874, 2998, 3350, and 8412). In the experiments with the vector that carried the human gene, which were initiated after the first two doses of the mouse gene experiments, we began with the "half dose" that proved effective with the mouse gene (animals 4954, 4984, 4826, and 4624) and later reduced to the "quarter dose" (2875, 5066, 5067). Some variations in the dose are also related to the volume it was possible to inject which was determined by conditions during surgery (detailed below in Surgical Procedure section).

Ethics and animal welfare. Experimental protocols were approved by the Volcani Center Institutional Animal Care and Use Committee and were conducted in accordance with principles outlined in the NIH Guide for the Care and Use of Laboratory Animals. For viral injections and electrophysiological recordings, animals were premedicated with acepromazine and pethidine, induced with propofol, and anesthetized and ventilated with isoflurane.

Construction and production of AAV5 vectors. The 2.1-kb human red/green opsin promoter[61,62] driving mouse (NCBI accession number NM_009918) or human (NCBI NM_001298) *CNGA3* cDNA was incorporated in AAV5 vectors, which were produced and purified by standard procedures[63] using an adenovirus-free, two-plasmid transfection system in 10-layer cell factories. Briefly, the two AAV5 vector plasmids were cotransfected into HEK-293 cells by $CaPO_4$ precipitation with the pXYZ packaging/helper plasmid containing the appropriate rep and cap genes. Cells were collected 60 hours post-transfection, pelleted, resuspended, and lysed. AAV5 was purified from the crude lysate using iodixanol gradients followed by fast protein liquid chromatography. The eluate was then desalted, concentrated, aliquoted, and stored at −80 °C. Viral titers were determined by quantitative competitive PCR assay relative to well-characterized AAV5 vector reference standards. Each vector preparation was examined for purity by resolution of the viral proteins on a sodium dodecyl sulfate-polyacrylamide gel and silver staining.

Surgical procedure: subretinal viral vector delivery. A minimally invasive procedure to introduce the viral vector into the subretinal space was developed (**Supplementary Figure S2**). Briefly, we used a micropipette attached to a syringe and inserted it through a single pars plana port, and then through the vitreous and via a small retinotomy into the subretinal space. Under direct visualization of an ophthalmic operating microscope, an assistant slowly injected the viral vector (suspended in BSS), creating a significant bleb of subretinal fluid. We strived to inject between 500–600 µl, but when the subretinal bleb neared the optic nerve, injection was stopped even if the full volume was not delivered. Vector dose (in viral genomes) as well as the volume injected in each eye are presented in **Table 1**. Thereafter, the micropipette was withdrawn and the scleral opening was sutured with a single 7-0 Vicryl suture. The surgically relevant features of the sheep eye and the surgical procedure are detailed in **Supplementary Figure S2**. In all animals, surgery was performed in the right eye, while the left eye served as an untreated control.

Following surgery, animals were treated with a topical chloramphenicol, polymyxin B and dexamethasone solution (Tarocidin-D; Taro, Haifa, Israel) three times daily for 1 week and monitored by an expert in sheep breeding and maintenance. Postoperative clinical and ophthalmological examinations were conducted regularly by board-certified ovine medicine and veterinary ophthalmology specialists over the whole term of the study.

Assessment of visual behavior and retinal function. Baseline testing was performed in all animals prior to surgery. Postoperative assessment was performed early (1–2 months postsurgery) in all animals to determine onset of effect, and then periodically thereafter with increasing intervals between the tests as the stability of the effect over time was established. Overall, both mouse and human gene-treated animals underwent similar numbers of maze and ERG tests per duration of follow-up, as can be seen in **Table 1**, at roughly similar intervals. Since treatment with the mouse gene was initiated before using the human gene, the follow up time for animals treated with the mouse gene was longer.

Behavioral assessment. Maze navigation testing was conducted as previously described.[19] Briefly, animals were directed to pass through a 9-m long maze with two barrier obstacles. A group of sheep positioned at the end of the maze attracted the test animal to pass through the maze as quickly as possible. For each animal, a test consisted of two successive trials, with the barriers randomly rearranged in their right–left orientation between trials to avoid a learning effect. Passage time and number of collisions with the obstacles were recorded for each trial. A trial lasted up to 30 seconds, and the maximal passage time of 30 seconds was ascribed to animals that failed to cross the maze.

Preoperative maze testing for *CNGA3*-mutant sheep (n = 17) was conducted in four sessions. Each preoperative session included three to five unaffected control sheep and three to five *CNGA3*-mutant sheep. Thirteen periodic post-treatment maze-testing sessions were conducted following m*CNGA3* (n = 8) or h*CNGA3* (n = 8) gene-augmentation treatments. One affected animal injected with BSS alone was also tested. Each of the post-treatment sessions included three to seven control unaffected sheep and three to seven treated *CNGA3*-mutant sheep. Some animals were tested in up to 11 post-treatment sessions, for as long as 37 months postoperatively (**Table 1**).

As only the right eye was treated in all cases, one session of maze testing was conducted with alternate patching of the treated and untreated eyes. Testing was conducted under daytime photopic (mean ± standard error illuminance of 1,349 ± 172 lux, LI-189 photometer, LI-COR, Lincoln, NE) and night-time scotopic conditions.

Raw and log-transformed values of passage time and number of collisions under either scotopic or photopic conditions were subjected to analysis of variance using the General Linear Model procedure of the Jump IN computer package (SAS Inst, Cary, NC). The statistical model for comparing performance of control unaffected sheep and untreated *CNGA3*-mutant sheep included the effects of genotype (unaffected or day blind), session (n = 4), gender, trial repetition number (n = 2), and age at time of testing, taken as covariates. The statistical model for comparing passage time and number of collisions before and after treatment in each individual sheep included the effects of treatment (unaffected, day blind before treatment, or day blind treated with either m*CNGA3* or h*CNGA3* AAV5 vectors) and animal nested within treatment. The statistical model for analyzing results of the test conducted with alternate eye patching included the effects of treatment (unaffected, or day blind treated with either m*CNGA3* or h*CNGA3* AAV5 vectors), eye-patch status (none, right eye, left eye) and trial repetition number. $P < 0.05$ was considered significant. Results are expressed as least squares means ± standard error.

ERG. Cone function was evaluated by full-field flash ERG, using a handheld mini Ganzfeld stimulator (HMsERG, Ocuscience, Henderson, NV) with a bandpass of 0.3–300 Hz. The recording protocol was as detailed in Ezra-Elia *et al.*[41] Briefly, following 10 minutes of light adaptation (30 cd/m^2), responses to four increasing intensities of stimulus (1, 2.5, 5, and 10 cd•s/m^2) were recorded. At each of the four stimulus intensities, a series of cone flicker responses to eight increasing frequencies (flashes presented at 10–80 Hz, with 128 responses averaged at each frequency) was recorded. Experimental animals were recorded preoperatively, 2 and 6 months postoperatively, and periodically thereafter for up to 32 months (**Table 1**). Flicker response amplitudes were measured between peak and trough. Where no flicker response was detected, a value of zero was inserted as the amplitude. The CFFF, or the highest frequency at which the animal could resolve flicker, was determined for each of the four intensities.

Differences between operated eye and fellow eye at different time points (pre- and postoperatively) were tested using the Wilcoxon nonparametric test. The repeated measures analysis of variance model was used to simultaneously assess the effects of eye (treated versus contralateral, untreated), time (baseline vs. first follow-up recording vs. second follow-up recording), CFFF, and the pairwise interactions between them. The Greenhouse-Geisser test was used to test the significance of the above effects. All statistical tests were two-tailed. $P < 0.05$ was considered significant.

Molecular genetic and histological analysis. Eyes of m*CNGA3*-treated, h*CNGA3*-treated, GFP reporter gene-injected, normal unaffected and untreated *CNGA3*-mutant sheep were studied. Animals were euthanized with 20% embutramide, 5% mebezonium iodide, and 0.5% tetracaine hydrochloride (0.1 ml/kg; T-61, Intervet Canada, Quebec, Canada), and both eyes were then enucleated.

Molecular genetic analysis. Retinas for molecular analysis were dissected from the enucleated eyes immediately after euthanasia, immersed in liquid nitrogen and kept at −80 °C until RNA extraction. mRNA was isolated from retinas using TRI-reagent (Sigma-Aldrich, St Louis, MO). cDNA was synthesized using the Verso cDNA kit (Thermo Scientific,

Waltham, MA) in accordance with the manufacturer's protocol. PCR-specific primers (**Supplementary Table S1**) were designed with Primer 3 to uniquely amplify sheep, mouse and human *CNGA3* mRNA. PCR was performed in a 30-µl reaction with 35 cycles. Sanger sequencing of PCR-purified products was used to verify the sequence of the endogenous mouse, human and sheep *CNGA3* genes.

Histology and immunohistchemistry. Eyes for histology and immunohistochemistry were fixed in Davidson solution. In each eye, a nasotemporal strip, 5 mm wide and crossing the center of the optic nerve, was cut, dehydrated, and embedded in paraplast (Leica Biosystems, Nussloch, Germany). From each strip, 4-µm sections were cut and every seventh section was stained with hematoxylin and eosin. For immunohistochemistry, deparaffinized sections from each eye were incubated in a decloaking chamber (Biocare Medical, Concord, CA) with 10 mmol/l citrate buffer (pH 6.0) at 125 °C, blocked with PBS solution containing 1% bovine serum albumin, 0.1% Triton X-100, and 10% normal donkey serum, and subsequently incubated overnight at 4 °C with one of the following primary antibodies: anti-*CNGA3* (goat polyclonal, 1:50; Santa Cruz Biotechnology, Santa Cruz, CA), anti-red/green opsin (rabbit polyclonal, 1:100; Chemicon International, Billerica, MA) or anti-GFP, conjugated with fluorescein isothiocyanate (mouse monoclonal, 1:100; Santa Cruz Biotechnology). After washing, the appropriate secondary antibody was applied for 1 hour: DyLight 488 donkey anti-rabbit or rhodamine red-X-conjugated donkey anti-goat IgG (1:250; both from Jackson ImmunoResearch Laboratories, West Grove, PA). Nuclei were counterstained with 4′,6-diamidino-2-phenylindole-containing mounting medium (Vector Laboratories, Burlingame, CA). To determine the specificity of the antigen–antibody reaction, corresponding negative controls were performed with secondary antibody alone. Photomicrography was performed using a fluorescent microscope (Olympus BX41; Olympus Corporation, Tokyo, Japan) equipped with a DP70 color digital camera.

SUPPLEMENTARY MATERIAL

Figure S1. Ocular function and structure in *CNGA3* achromatopsia (ACHM) patients.

Figure S2. Comparative anatomy of the sheep eye and development of the surgical approach.

Figure S3. Subretinal injection of BSS alone does not provide behavioral or functional rescue.

Figure S4. Retinal structure is preserved following subretinal injection.

Table S1. Primer sequences used to amplify CNGA3 DNA.

Movie S1. Photopic maze testing of day-blind sheep following *CNGA3* gene augmentation therapy.

ACKNOWLEDGMENTS

The authors thank Tali Bdolah-Abram for her help with statistical analysis of the data, and Cila Ganot and Dafna Gootwine for video recording of the maze tests. This study was supported (in part) by a grant from the US-Israel Binational Science Foundation, the Chief Scientist Office of the Israeli Ministry of Health and by the Macula Vision Research Foundation, as well as by unrestricted awards from The Joseph Alexander Foundation and Yedidut 1 Research Grant. E.B., E.G., R.O., and W.W.H. participated in the study design; E.B., E.G., R.O., A.O., and R.E.E. analyzed the data; E.B., E.G., A.O., R.E.E., E.A., and R.O. wrote the manuscript; E.G. and A.R. bred and provided the affected sheep and collected sheep samples; E.G. and A.R. planned and conducted the behavioral tests; A.O. performed histological and immunohistochemical examinations; R.E.E. planned, conducted and analyzed the electroretinographic recordings; A.E., L.Z., and D.S. performed and analyzed the molecular genetics experiments; H.H. and A.R. performed anesthesia for the surgical and clinical procedures and provided veterinary surveillance; E.A. developed the surgical technique and performed all surgeries; E.Y. assisted in the retinal surgeries; W.W.H. designed and constructed all of the AAV vectors used in this study; R.O. conducted the ophthalmic examinations. W.W.H. and the University of Florida have a financial interest in the use of AAV therapies.

REFERENCES

1. Roosing, S, Thiadens, AA, Hoyng, CB, Klaver, CC, den Hollander, AI and Cremers, FP (2014). Causes and consequences of inherited cone disorders. *Prog Retin Eye Res* **42**: 1–26.
2. Simunovic, MP and Moore, AT (1998). The cone dystrophies. *Eye (Lond)* **12 (Pt 3b)**: 553–565.
3. Kohl, S, Marx, T, Giddings, I, Jägle, H, Jacobson, SG, Apfelstedt-Sylla, E *et al.* (1998). Total colourblindness is caused by mutations in the gene encoding the alpha-subunit of the cone photoreceptor cGMP-gated cation channel. *Nat Genet* **19**: 257–259.
4. Wissinger, B, Gamer, D, Jägle, H, Giorda, R, Marx, T, Mayer, S *et al.* (2001). CNGA3 mutations in hereditary cone photoreceptor disorders. *Am J Hum Genet* **69**: 722–737.
5. Winick, JD, Blundell, ML, Galke, BL, Salam, AA, Leal, SM and Karayiorgou, M (1999). Homozygosity mapping of the Achromatopsia locus in the Pingelapese. *Am J Hum Genet* **64**: 1679–1685.
6. Kohl, S, Baumann, B, Broghammer, M, Jägle, H, Sieving, P, Kellner, U *et al.* (2000). Mutations in the CNGB3 gene encoding the beta-subunit of the cone photoreceptor cGMP-gated channel are responsible for achromatopsia (ACHM3) linked to chromosome 8q21. *Hum Mol Genet* **9**: 2107–2116.
7. Kohl, S, Varsanyi, B, Antunes, GA, Baumann, B, Hoyng, CB, Jägle, H *et al.* (2005). CNGB3 mutations account for 50% of all cases with autosomal recessive achromatopsia. *Eur J Hum Genet* **13**: 302–308.
8. Thiadens, AA, Slingerland, NW, Roosing, S, van Schooneveld, MJ, van Lith-Verhoeven, JJ, van Moll-Ramirez, N *et al.* (2009). Genetic etiology and clinical consequences of complete and incomplete achromatopsia. *Ophthalmology* **116**: 1984–9.e1.
9. Zelinger, L, Cideciyan, AV, Kohl, S, Schwartz, SB, Rosenmann, A, Eli, D *et al.* (2015). Genetics and Disease Expression in the CNGA3 Form of Achromatopsia: Steps on the Path to Gene Therapy. *Ophthalmology* **122**: 997–1007.
10. Li, S, Huang, L, Xiao, X, Jia, X, Guo, X and Zhang, Q (2014). Identification of CNGA3 mutations in 46 families: common cause of achromatopsia and cone-rod dystrophies in Chinese patients. *JAMA Ophthalmol* **132**: 1076–1083.
11. Liang, X, Dong, F, Li, H, Li, H, Yang, L and Sui, R (2015). Novel CNGA3 mutations in Chinese patients with achromatopsia. *Br J Ophthalmol* **99**: 571–576.
12. Kohl, S, Baumann, B, Rosenberg, T, Kellner, U, Lorenz, B, Vadalà, M *et al.* (2002). Mutations in the cone photoreceptor G-protein alpha-subunit gene GNAT2 in patients with achromatopsia. *Am J Hum Genet* **71**: 422–425.
13. Thiadens, AA, den Hollander, AI, Roosing, S, Nabuurs, SB, Zekveld-Vroon, RC, Collin, RW *et al.* (2009). Homozygosity mapping reveals PDE6C mutations in patients with early-onset cone photoreceptor disorders. *Am J Hum Genet* **85**: 240–247.
14. Kohl, S, Coppieters, F, Meire, F, Schaich, S, Roosing, S, Brennenstuhl, C *et al.*; European Retinal Disease Consortium. (2012). A nonsense mutation in PDE6H causes autosomal-recessive incomplete achromatopsia. *Am J Hum Genet* **91**: 527–532.
15. Yeh, CY, Goldstein, O, Kukekova, AV, Holley, D, Knollinger, AM, Huson, HJ *et al.* (2013). Genomic deletion of CNGB3 is identical by descent in multiple canine breeds and causes achromatopsia. *BMC Genet* **14**: 27.
16. Sidjanin, DJ, Lowe, JK, McElwee, JL, Milne, BS, Phippen, TM, Sargan, DR *et al.* (2002). Canine CNGB3 mutations establish cone degeneration as orthologous to the human achromatopsia locus ACHM3. *Hum Mol Genet* **11**: 1823–1833.
17. Pang, JJ, Alexander, J, Lei, B, Deng, W, Zhang, K, Li, Q *et al.* (2010). Achromatopsia as a potential candidate for gene therapy. *Adv Exp Med Biol* **664**: 639–646.
18. Komáromy, AM, Alexander, JJ, Rowlan, JS, Garcia, MM, Chiodo, VA, Kaya, A *et al.* (2010). Gene therapy rescues cone function in congenital achromatopsia. *Hum Mol Genet* **19**: 2581–2593.
19. Shamir, MH, Ofri, R, Bor, A, Brenner, O, Reicher, S, Obolensky, A *et al.* (2010). A novel day blindness in sheep: epidemiological, behavioural, electrophysiological and histopathological studies. *Vet J* **185**: 130–137.
20. Reicher, S, Seroussi, E and Gootwine, E (2010). A mutation in gene CNGA3 is associated with day blindness in sheep. *Genomics* **95**: 101–104.
21. Carvalho, LS, Xu, J, Pearson, RA, Smith, AJ, Bainbridge, JW, Morris, LM *et al.* (2011). Long-term and age-dependent restoration of visual function in a mouse model of CNGB3-associated achromatopsia following gene therapy. *Hum Mol Genet* **20**: 3161–3175.
22. Michalakis, S, Mühlfriedel, R, Tanimoto, N, Krishnamoorthy, V, Koch, S, Fischer, MD *et al.* (2010). Restoration of cone vision in the CNGA3-/- mouse model of congenital complete lack of cone photoreceptor function. *Mol Ther* **18**: 2057–2063.
23. Michalakis, S, Mühlfriedel, R, Tanimoto, N, Krishnamoorthy, V, Koch, S, Fischer, MD *et al.* (2012). Gene therapy restores missing cone-mediated vision in the CNGA3-/- mouse model of achromatopsia. *Adv Exp Med Biol* **723**: 183–189.
24. Pang, JJ, Deng, WT, Dai, X, Lei, B, Everhart, D, Umino, Y *et al.* (2012). AAV-mediated cone rescue in a naturally occurring mouse model of CNGA3-achromatopsia. *PLoS One* **7**: e35250.
25. Alexander, JJ, Umino, Y, Everhart, D, Chang, B, Min, SH, Li, Q *et al.* (2007). Restoration of cone vision in a mouse model of achromatopsia. *Nat Med* **13**: 685–687.
26. Mancuso, K, Hauswirth, WW, Li, Q, Connor, TB, Kuchenbecker, JA, Mauck, MC *et al.* (2009). Gene therapy for red-green colour blindness in adult primates. *Nature* **461**: 784–787.
27. Shinozaki, A, Hosaka, Y, Imagawa, T and Uehara, M (2010). Topography of ganglion cells and photoreceptors in the sheep retina. *J Comp Neurol* **518**: 2305–2315.
28. Hauswirth, WW, Aleman, TS, Kaushal, S, Cideciyan, AV, Schwartz, SB, Wang, L *et al.* (2008). Treatment of leber congenital amaurosis due to RPE65 mutations by ocular subretinal injection of adeno-associated virus gene vector: short-term results of a phase I trial. *Hum Gene Ther* **19**: 979–990.
29. Acland, GM, Aguirre, GD, Ray, J, Zhang, Q, Aleman, TS, Cideciyan, AV *et al.* (2001). Gene therapy restores vision in a canine model of childhood blindness. *Nat Genet* **28**: 92–95.
30. Acland, GM, Aguirre, GD, Bennett, J, Aleman, TS, Cideciyan, AV, Bennicelli, J *et al.* (2005). Long-term restoration of rod and cone vision by single dose rAAV-mediated gene transfer to the retina in a canine model of childhood blindness. *Mol Ther* **12**: 1072–1082.

31. Narfström, K, Vaegan, Katz, M, Bragadottir, R, Rakoczy, EP and Seeliger, M (2005). Assessment of structure and function over a 3-year period after gene transfer in RPE65-/- dogs. *Doc Ophthalmol* **111**: 39–48.
32. Mühlfriedel, R, Tanimoto, N and Seeliger, MW (2014). [Gene replacement therapy in achromatopsia type 2]. *Klin Monbl Augenheilkd* **231**: 232–240.
33. Boye, SE, Boye, SL, Lewin, AS and Hauswirth, WW (2013). A comprehensive review of retinal gene therapy. *Mol Ther* **21**: 509–519.
34. Cideciyan, AV (2010). Leber congenital amaurosis due to RPE65 mutations and its treatment with gene therapy. *Prog Retin Eye Res* **29**: 398–427.
35. MacLaren, RE, Groppe, M, Barnard, AR, Cottriall, CL, Tolmachova, T, Seymour, L *et al.* (2014). Retinal gene therapy in patients with choroideremia: initial findings from a phase ½ clinical trial. *Lancet* **383**: 1129–1137.
36. Sahel, JA and Roska, B (2013). Gene therapy for blindness. *Annu Rev Neurosci* **36**: 467–488.
37. Komáromy, AM, Rowlan, JS, Corr, AT, Reinstein, SL, Boye, SL, Cooper, AE *et al.* (2013). Transient photoreceptor deconstruction by CNTF enhances rAAV-mediated cone functional rescue in late stage CNGB3-achromatopsia. *Mol Ther* **21**: 1131–1141.
38. Sundaram, V, Wilde, C, Aboshiha, J, Cowing, J, Han, C, Langlo, CS *et al.* (2014). Retinal structure and function in achromatopsia: implications for gene therapy. *Ophthalmology* **121**: 234–245.
39. Dubis, AM, Cooper, RF, Aboshiha, J, Langlo, CS, Sundaram, V, Liu, B *et al.* (2014). Genotype-dependent variability in residual cone structure in achromatopsia: toward developing metrics for assessing cone health. *Invest Ophthalmol Vis Sci* **55**: 7303–7311.
40. Maguire, AM, Simonelli, F, Pierce, EA, Pugh, EN Jr, Mingozzi, F, Bennicelli, J *et al.* (2008). Safety and efficacy of gene transfer for Leber's congenital amaurosis. *N Engl J Med* **358**: 2240–2248.
41. Ezra-Elia, R, Banin, E, Honig, H, Rosov, A, Obolensky, A, Averbukh, E *et al.* (2014). Flicker cone function in normal and day blind sheep: a large animal model for human achromatopsia caused by CNGA3 mutation. *Doc Ophthalmol* **129**: 141–150.
42. Polat, U (2008). Restoration of underdeveloped cortical functions: evidence from treatment of adult amblyopia. *Restor Neurol Neurosci* **26**: 413–424.
43. Rizzo, S, Belting, C, Cinelli, L, Allegrini, L, Genovesi-Ebert, F, Barca, F *et al.* (2014). The Argus II Retinal Prosthesis: 12-month outcomes from a single-study center. *Am J Ophthalmol* **157**: 1282–1290.
44. Renier, L, De Volder, AG and Rauschecker, JP (2014). Cortical plasticity and preserved function in early blindness. *Neurosci Biobehav Rev* **41**: 53–63.
45. Cideciyan, AV, Hauswirth, WW, Aleman, TS, Kaushal, S, Schwartz, SB, Boye, SL *et al.* (2009). Vision 1 year after gene therapy for Leber's congenital amaurosis. *N Engl J Med* **361**: 725–727.
46. Cideciyan, AV, Aguirre, GK, Jacobson, SG, Butt, OH, Schwartz, SB, Swider, M *et al.* (2015). Pseudo-fovea formation after gene therapy for RPE65-LCA. *Invest Ophthalmol Vis Sci* **56**: 526–537.
47. Ashtari, M, Cyckowski, LL, Monroe, JF, Marshall, KA, Chung, DC, Auricchio, A *et al.* (2011). The human visual cortex responds to gene therapy-mediated recovery of retinal function. *J Clin Invest* **121**: 2160–2168.
48. Ashtari, M, Cyckowski, L, Yazdi, A, Viands, A, Marshall, K, Bókkon, I *et al.* (2014). fMRI of retina-originated phosphenes experienced by patients with Leber congenital amaurosis. *PLoS One* **9**: e86068.
49. Dilks, DD, Julian, JB, Peli, E and Kanwisher, N (2014). Reorganization of visual processing in age-related macular degeneration depends on foveal loss. *Optom Vis Sci* **91**: e199–e206.
50. Palmer, S, Logan, D, Nabili, S and Dutton, GN (2010). Effective rehabilitation of reading by training in the technique of eccentric viewing: evaluation of a 4-year programme of service delivery. *Br J Ophthalmol* **94**: 494–497.
51. Khan, NW, Wissinger, B, Kohl, S and Sieving, PA (2007). CNGB3 achromatopsia with progressive loss of residual cone function and impaired rod-mediated function. *Invest Ophthalmol Vis Sci* **48**: 3864–3871.
52. Thiadens, AA, Roosing, S, Collin, RW, van Moll-Ramirez, N, van Lith-Verhoeven, JJ, van Schooneveld, MJ *et al.* (2010). Comprehensive analysis of the achromatopsia genes CNGA3 and CNGB3 in progressive cone dystrophy. *Ophthalmology* **117**: 825–30.e1.
53. Genead, MA, Fishman, GA, Rha, J, Dubis, AM, Bonci, DM, Dubra, A *et al.* (2011). Photoreceptor structure and function in patients with congenital achromatopsia. *Invest Ophthalmol Vis Sci* **52**: 7298–7308.
54. Fahim, AT, Khan, NW, Zahid, S, Schachar, IH, Branham, K, Kohl, S *et al.* (2013). Diagnostic fundus autofluorescence patterns in achromatopsia. *Am J Ophthalmol* **156**: 1211–1219.e2.
55. Cassar, SC, Chen, J, Zhang, D and Gopalakrishnan, M (2004). Tissue specific expression of alternative splice forms of human cyclic nucleotide gated channel subunit CNGA3. *Mol Vis* **10**: 808–813.
56. Dai, G, Sherpa, T and Varnum, MD (2014). Alternative splicing governs cone cyclic nucleotide-gated (CNG) channel sensitivity to regulation by phosphoinositides. *J Biol Chem* **289**: 13680–13690.
57. Kaupp, UB and Seifert, R (2002). Cyclic nucleotide-gated ion channels. *Physiol Rev* **82**: 769–824.
58. Biel, M and Michalakis, S (2007). Function and dysfunction of CNG channels: insights from channelopathies and mouse models. *Mol Neurobiol* **35**: 266–277.
59. Ding, XQ, Harry, CS, Umino, Y, Matveev, AV, Fliesler, SJ and Barlow, RB (2009). Impaired cone function and cone degeneration resulting from CNGB3 deficiency: down-regulation of CNGA3 biosynthesis as a potential mechanism. *Hum Mol Genet* **18**: 4770–4780.
60. Xu, J, Morris, L, Fliesler, SJ, Sherry, DM and Ding, XQ (2011). Early-onset, slow progression of cone photoreceptor dysfunction and degeneration in CNG channel subunit CNGB3 deficiency. *Invest Ophthalmol Vis Sci* **52**: 3557–3566.
61. Nathans, J, Thomas, D and Hogness, DS (1986). Molecular genetics of human color vision: the genes encoding blue, green, and red pigments. *Science* **232**: 193–202.
62. Wang, Y, Macke, JP, Merbs, SL, Zack, DJ, Klaunberg, B, Bennett, J *et al.* (1992). A locus control region adjacent to the human red and green visual pigment genes. *Neuron* **9**: 429–440.
63. Zolotukhin, S, Potter, M, Zolotukhin, I, Sakai, Y, Loiler, S, Fraites, TJ Jr *et al.* (2002). Production and purification of serotype 1, 2, and 5 recombinant adeno-associated viral vectors. *Methods* **28**: 158–167.